

PROCEEDINGS OF SPIE

[SPIDigitalLibrary.org/conference-proceedings-of-spie](https://spiedigitallibrary.org/conference-proceedings-of-spie)

Optical channeling for radial holographic grating recording in chalcogenide glassy semiconductors films and photo-thermo-plastic films

N. Kukhtarev, T. Kukhtareva, S. Bairavarasu, V. Edwards, J. Wang, et al.

N. Kukhtarev, T. Kukhtareva, S. Bairavarasu, V. Edwards, J. Wang, V. Rotaru, P. Buchhave, "Optical channeling for radial holographic grating recording in chalcogenide glassy semiconductors films and photo-thermo-plastic films," Proc. SPIE 5912, Operational Characteristics and Crystal Growth of Nonlinear Optical Materials II, 591209 (20 September 2005); doi: 10.1117/12.614173

SPIE.

Event: Optics and Photonics 2005, 2005, San Diego, California, United States

Optical Channeling For Radial Holographic Grating Recording In Chalcogenide Glassy Semiconductors Films and Photo-thermo-plastic films

N.Kukhtarev, T. Kukhtareva, S.Bairavarasu, V.Edwards, J. Wang, Phys. Dep., Alabama A&M University

V.Rotaru, Dept. of Physics, Moldova State Univ., 60 A.Mateevici str., Chisinau, MD-2009, Moldova,

P.Buchhave, Department of Physics,DTU, Lyngby 2800, Denmark

Abstract

We discuss phenomena of the optical photons and charged particle channeling in the periodic structures. While particle (as protons) channeling is widely used for the characterization of defects in crystals, channeling of photons is less known. We have demonstrated feasibility of optical channeling method for copying of phase radial grating on the chalcogenide semiconductor glass film and photo-thermoplastic films (PTPF). Chalcogenide glassy semiconductors (CGS) as a medium for recording of optical information have some advantages such as the possibility of achieving a higher resolution power, stability, and a high photosensitivity. We report about recording of the radial phase grating in the doped As-S-Se (CGS). Radial grating was recorded by making copy from the master phase grating placed in the near-field zone and exposure to the CW green ($\lambda=532$ nm) low power ($P=100$ mW) solid-state laser or incoherent UV source. The exposure time has been varied from 15 to 30 min. The recording process could be explained by optical channeling. This phenomenon gives us an opportunity to create phase radial grating using coherent and incoherent illumination.

1. INTRODUCTION

Channeling of charged particles (electrons, protons) in crystals is commonly used in material science for characterization of crystals defects and impurities [1-2]. On the other hand, channeling of photons by periodic structures is less known. It has been shown, that a volume phase grating with a period greater than the wavelength of light can localize light near the planes having the maximum value of refractive index [3-5]. The similarity between charged particle and photon channeling stems out from analogy between Maxwell equation and the Schrodinger equations that describe propagation of photon and ion beams in coherent channeling. Optical periodic structures can be formed in the crystals by recording of interference pattern in photorefractive materials. It was shown in the paper [6], that holographic grating, recorded in the photorefractive crystal $\text{LiNbO}_3:\text{Fe}$ produce efficient electric-field grating. This electric field grating may introduce periodic stress modulation in the crystal lattice and in this way influence also proton channeling. Experimentally this influence was demonstrated in the paper [6], by channeling of 1.03 MeV protons in the (0001) plane of an x-cut $\text{LiNbO}_3 : \text{Fe}$ crystal. The channel is observed to be narrower in a region of the crystal where a holographic electric field grating has been recorded. The channel observed from the region periodically strained by the spatially alternating persistent internal electric fields of the holograms is about 0.3 degree narrower than that observed from the neutral zone. Angular half-width of the channeling distribution was about 2 degrees. The results here seen to be a superposition of the channel narrowing from the holographic grating electric field applied alternatively in the positive and negative directions. The observed narrowing of ion beam channeling in $\text{LiNbO}_3: \text{Fe}$ holographic strain fields is much larger than expected from changes in lattice constants. This example show interrelation between optically induced periodic structures and crystal lattice parameters, manifested in ion channeling. Channeling of neutral particles (as neutrons) and photons in crystals was reviewed in the paper [7], where effects of spin waves, elastic waves and domain walls on channeling are examined.

Recently predicted and observed [8] deuteron acceleration in ferroelectric crystals LiTaO₃ in the external electric field along the C-axis may be also affected by the channeling effects. In the external ac (50 Hz) field of 75 KV/cm the neutron emission attributed to D-D fusion was 0.5 neutrons/s. This gives the fusion rate $7.8 \cdot 10^{-21}$ 1/s per deuteron pair that is two order of magnitude higher the Jones level. It was also demonstrated, that holographic grating recorded in LiNbO₃: Fe crystal may be also used for channeling of photons [9] that allow visualizing periodic distribution of refractive index. This effect, allow us to use optical channeling for copying of phase gratings, including those with two-dimensional refractive index modulation.

In the next section we will discuss theoretical model of the optical channeling by periodic modulation of the refractive index (by phase grating). Experimental realization of such optical channeling will be demonstrated for copying of phase radial grating on chalcogenide semiconductor film and described in the experimental section.

II. THEORETICAL MODELING OF OPTICAL CHANNELING

A transversal modulation of refractive index of the thick crystal may be regarded as recording of bunch of optical channels or wave-guides. As it was shown in [10], a modulation of refractive index may be visualized in the near field by optical channeling. We can model a transversal modulation of the dielectric constant by the function

$$\varepsilon(x, y) = \varepsilon_0 + \varepsilon_x \cos q_x x + \varepsilon_y \cos(q_y y + \varphi) \quad (1)$$

with ε_0 average value, and $\varepsilon_{x,y}$ are the amplitude of modulation alone transverse x and y axis, with wave numbers q_x , q_y respectively, and proper phase shift φ . Introducing the function $\varepsilon(x, y)$ in Maxwell equation, we can get result [4] for the near-field intensity as [4]:

$$I = I_0 \left\{ 1 + \varepsilon_x \left(\frac{L_x}{\lambda} \right)^2 \sin^2 \left(\frac{\pi \lambda z}{2 L_x^2} \right) \cos q_x x + \varepsilon_y \left(\frac{L_y}{\lambda} \right)^2 \sin^2 \left(\frac{\pi \lambda z}{2 L_y^2} \right) \cos(q_y y + \varphi) \right\} \quad (2)$$

where $L_{x,y} = 2\pi/q_{x,y}$. The solution (2) is valid for a small modulation and includes a longitudinal modulation with the periods

$$z_{x,y} = \frac{2 L_{x,y}^2}{\lambda} \quad (3)$$

For experimental values with KNbO₃ ($\lambda = 0.514 \mu\text{m}$, $L_x = L_y = 35 \mu\text{m}$) we can get for longitudinal period $z_x = z_y = 0.49 \text{ cm}$ that is very close to experimental value of 0.5 cm [4].

3. EXPERIMENTAL REALIZATION OF RADIAL GRATING COPYING IN CHALCOGENIDE GLASSES AND PTPM.

3.1 PHOTO-THERMO- PLASTIC MATERIALS

Photo-thermoplastic films (PTPF) are non-silver two-layered structures for optical data recording [11]. Semiconductor-thermoplastic configuration provides recording of photographic, holographic, and other types of optical data without a wet chemical development, giving ones the better radiation resistance. Optical data recorded on photo-thermoplastic (PTP) media is characterized by simplicity of development and erasing processes; unlike xerography it does not need any special developing material; unlike CCDs it does not need any complex electronic interface. The property of radiation resistance makes these systems particularly useful for remote sensing of different objects from Space.

Usually PTPF contains several more layers for improving of its parameters. The first layer is an adhesive one, which is deposited on polymer substrate. The second layer is semitransparent electrode. The third

layer is being deposited upon the electrode and is in charge of electron injection. The fourth layer is a barrier one, often represents by a heterojunction, and then transport layer is followed. As previous investigations showed (see Ref. [12]), the semiconductor layer weakly affect photographic parameters of PTPF.

Visualizing layer (thermoplastic) could also be modified. Alteration of the type of the used polymers, their additional doping, creation of visualizing multi-layers, and changing of the surface properties of thermoplastic layer allows varying of thermo-development regimes, i.e. temperature diapason and potential of charging while the optical data record [13].

3.2 PARAMETERS OF GLASSY CHALCOGENIDE LAYERS

The variety of the constructions of charging devices is dictated by the purposes of a particular recording device. A successful explanation of the optimal regimes for each type of the charging device has been found. Collected data is being used for PTP recording and also to predict the behavior of the surface potential $V_s(t)$ on PTPM using characteristics of the known charging devices.

Kinetics of the surface potential V_s at the stage of charging of the photosensitive layer of As_2S_3 , As_2Se_3 , and their solid solutions proves a complex nature of the processes inside the material. It was rigorously studied for the different corona producing devices of different efficiency. With the growth of the potential the maximum appears on the curves of $V_s(t)$. The subsequent decreasing of V_s we tend to connect with the growth of the space charge at the lower levels. The screening of the surface potential by this charge leads to apparent decreasing of the effective thickness of the layer. In this case, the surface potential V_s , determining the light sensitivity of PTPM, is formed by the charge, accumulated on the surface and inside the bulk of the layers as well as in between them. Using such simple model, the effective deepness b of the charge bedding and their amount N were calculated.

For the As_2Se_3 layers with thickness $d=2.4 \mu m$, the values b and N were: $b=1.5 \mu m$, $N=2 \cdot 10^{17} cm^{-3}$. For the layers consisting of the solid solution $(As_2Se_3)_{0.7}(As_2S_3)_{0.3}$ and $d=3.0 \mu m$, these values were $1.9 \mu m$ and $3 \cdot 10^{17} cm^{-3}$ correspondingly, and for As_2S_3 layer with thickness $d=2.2 \mu m$ the corresponding values were: $b=1.6 \mu m$ and $N=7 \cdot 10^{17} cm^{-3}$. These values of the accumulated charge concentrations are in good agreement with the values of densities of localized states in these materials. The growth of illumination is increasing the field of predominant of the bedding of compensating charge that leads to the more pronounced maximum on the $V_s(t)$ curve. Such dependence is not observed at the temperature growth up to $80^\circ C$ that means that effective deepness of charge bedding is not changed in this case.

A number of requirements have to be met in the process of fabrication of PTPF based on chalcogenide glasses. Among them are high specific resistance (10^{13} - $10^{14} Ohm \cdot cm$), dark conductivity is of less importance), mechanical durability, thermal stability of electro-physical parameters and recycling of the used materials. The basic requirements to the photosensitive semiconductor layers affiliated to the PTPF structure are their high resistance and large multiplication ratio of resistance change under the electromagnetic irradiation exposure. In spite of the successes in development of electro-photography and PTP recording on the base of the materials mentioned above, currently there are remained the actual tasks of photosensitivity increasing, widening of spectral range for recording, and realization of new properties of media for information recording. For its successful application in two-layer PTPF photosensitive semiconductor layer should have dark resistivity about $\rho_d \sim 10^{12}$ - $10^{14} Ohm \cdot cm$ at the multiplication ratio of photo-response at the level of 10 at the minimal illumination of 5-10 Lx. Modification of composition allows purposeful changing of the properties of thin films and obtaining the layers, satisfying the requirements of any practical needs. Also, one of the important tasks in the field of recording of optical information from space is the search of the materials of recording media, possessing high photosensitivity and transparency for polychromatic light including monochromic light of definite wavelength.

Comparison of the properties (see Fig.1) was carried out in accordance with the following procedure. At the same graphs there were built the dependences of transmission $T(\%)=f(\lambda)$ and long-wave decay of the photocurrent $I_p(\%)=f(\lambda)$ for thin films of different composition. With account of peculiarities of the photo-effect in thin layers of chalcogenide glass semiconductors, mentioned in [14] the photocurrent was measured at the negative polarity of illuminated electrode. At the comparison of solid solutions the relative values of photocurrent were put in Y-direction. Values themselves had been determined in accordance with formula

$$I_p(\%) = \frac{I_p}{I_{p \max}} \cdot 100\%$$

Here I_p is the absolute value of photocurrent at the given wavelength of descending light, $I_{p \max}$ – maximal value of photocurrent for given material. The projection of point intersection of T and I_p curves on the axis of wavelengths λ gives ones the optimal wavelength of the descending light λ^{\max} at which material is satisfying to the requirement of largest sensitivity and transparency. Hence, the carried out comparison of the properties of thin films of solid solutions system $(As_2S_3)_x(As_2Se_3)_{1-x}$ has shown the opportunity to choose the thin film composition, which can be used in the different devices for information recording.

Measurement of the drift mobility of charge carriers was carried out through the time-flight method [15] on “sandwich” type samples with deposited chromic top electrode. The values of band gap width determined from the curves of adsorption in coordinates $(h\nu K)^{1/2} = f(h\nu)$ and from the spectral characteristics of photoconductivity (by the wavelength of monochromatic light at which photocurrent decreases up to 50% of maximal value) are coincided. Width of the band gap is linearly decreased with the composition alteration from $E_g = 2.4$ eV (As_2S_3) to the value 1.75 eV (As_2Se_3). We determined that E_g values are practically congruent with values presented in Refs [16,17]. Dependence of the coefficients of adsorption of thin films $(As_2S_3)_x(As_2Se_3)_{1-x}$ on the photons energy of incident irradiation in the field of weak adsorption ($h\nu < E_g$), for x : 1 – 1.0; 2 – 0.7; 3 – 0.5; 4 – 0.3; 5 – 0 is presented in Fig.2.

Fig.2 shows that in the field of weak adsorption ($h\nu < E_g$) all compositions there have exponential dependence of adsorption coefficient on the energy of descending phonons as an evidence of Urbach’s law feasibility: $K = K_0 \exp [(h\nu - E_g)/\Delta]$. Feasibility of this rule, generally speaking, points to the presence of “tail” of state’s density in band gap. Charge carriers possess the greatest mobility in the layers As_2Se_3 ($\mu \sim 10^7$ cm²/Vc). As the arsenic sulfide content growths the drift mobility of carriers is decreased and achieved the value of $\mu \sim 10^{10}$ cm²/Vc in the case of $(As_2S_3)_{0.7}(As_2Se_3)_{0.3}$. Temperature dependence of the drift mobility has the exponent form: $\mu \sim \exp (-E_a/kT)$, where E_a is energy of activation of mobility. Dependence $\lg \mu = f(10^3/T)$ allows to find out the energy of trap’s activation which are participating in the charge transfer. Determined value of the activation energy E_a for arsenic selenide is 0.1 eV; for solid solutions E_a is increased up to 0.18 eV for the $(As_2S_3)_{0.7}(As_2Se_3)_{0.3}$ composition. The sensitivity spectra of the PTPF on base chalcogenide glass semiconductors are presented in Fig 3.

These results could be successfully applied to systems of photo-thermoplastic recording for creation of PTPF from $(As_2S_3)_{0.5}(As_2Se_3)_{0.5}$ layers and heterojunctions on their base; however, the high speed of the relaxation of the dark surface potential limits their application in simultaneous recording procedure. The performed investigations allow determining the composition in doped As-S-Se systems with different percentage of containing component, possessing high exploiting parameters. Studying of optical, photoelectrical, and electro-photographical properties of As-S-Se-Sn compounds shows that these layers possess darkish specific resistance of $3 \cdot 5 \cdot 10^{14}$ Ohm·cm at $T = 30^\circ\text{C}$, and the changing brevity of resistance is $K = 10^2$ at $E = 10$ lx. When the temperature rises up to the values used during PTP recording ($\sim 70^\circ\text{C}$), an insignificant deterioration of chalcogenide semiconductor parameters occurs. Maximum of spectral sensitivity of such layers is dependent on the layer composition and located within the range 460–480 nm in which multiplicity of the photo-response $(1.8\text{--}11) \cdot 10^3$ is ensured. When He-Ne laser ($\lambda = 630$ nm) is used, the photo-response multiplicity constitutes from 20 to 70 while irradiation power is 10^{-5} W/cm². These compositions can be used for creation of PTPM with sensitivity from $1.4 \cdot 10^{-6}$ to 10^{-5} A/W. Thermal dependence of the conductivity of multi-component chalcogenide thin layers for temperature range 310–360 K and applied electric field is shown in Fig.4. For the first time there were obtained photosensitive layers with $\rho_d \sim 7 \cdot 10^{14}$ Ohm·cm and $K = 30$ at the power of incident irradiation $8 \cdot 10^{-7}$ W. These layers, according to their sensibility, are close to traditional in electro-photographical selenium plates, thermally stable and can be applied for both simultaneous and consequent procedures of optical information recording; moreover, they possess high transparency ($T = 90\%$ at $\lambda = 630$ nm). These results allow to conclusion that these layers can be successfully used for preparation of two-layer PTPF capable to register optical information in diapason 400–700 nm. Studying of influence of electric field polarity on photocurrent and on light response showed that maximum values reach when negative potential applied to alight surface of thin CGS layers.

Using PTPF production on a base of CGS thin films, we ensure that their spectral sensitivity covers X-rays, visible, and near-IR ranges. Also, one can select a wavelength range with a width of about 0.1 μm in which some of PTPFs are able to ensure photographing of objects in these spectral zones. Technologically, these CGS layers were created on flexible 40-m-long and 190-mm-wide films with thickness accuracy of better than 0.2 nm and electric parameters deviations not more than $\pm 5\%$.

Chalcogenide glassy semiconductors (CGS) as a medium for recording of optical information have some advantages such as the possibility of achieving a higher resolution power, stability, and a high photosensitivity. We report about recording of the radial phase grating in the doped As-S-Se CGS. Radial grating was recorded by making copy from the master phase grating placed in the near-field zone and exposure to the CW green ($\lambda=532\text{ nm}$) low power ($P=100\text{ mW}$) solid-state laser or incoherent UV source. The exposure time has been varied from 15 to 30 min.

4. Experimental realization of radial grating copying in chalcogenide glasses.

Chalcogenide glassy semiconductors (CGS) as a medium for recording of optical information have some advantages such as the possibility of achieving a higher resolution power, stability, and a high photosensitivity. We report about recording of the radial phase grating in the doped As-S-Se CGS. Radial grating was recorded by making copy from the master phase grating placed in the near-field zone and exposure to the CW green ($\lambda=532\text{ nm}$) low power ($P=100\text{ mW}$) solid-state laser or incoherent UV source. The exposure time has been varied from 15 to 30 min. The diffraction efficiency of the copied gratings was between 1,8 % and 4,3 %. By selective chemical etching the diffraction efficiency of the holographic copies was increased until 8-12 times. The recording process could be explained by optical channeling. This phenomenon gives us an opportunity to create phase radial grating using coherent and incoherent illumination. On the Fig.5 is shown photo of radial grating, recorded in CGS, and PTPF using above described optical channeling method. The patterns of diffraction orders for master radial element and CGS -type element is presented on the Fig. 6 (a,b). Optical scheme of moving-grating interferometer and example of interference pattern, created by the radial grating are shown on the Fig 5 and Fig.7.

4.1 FOR THE CENTRAL SPOT OF THE DIFFRACTION PATTERN:

1. For PTPM type of diffraction grating material the intensity of incident light was approximately 15mw and the output intensity 6mw. For this PTP material when one particular spot was exposed to He-Ne laser the output intensity is maximum and gradually reduces, however if the incident beam is blocked for some time and same spot is again exposed to laser light the output Intensity is again maximum and gradually reduces.
2. For CSG type of diffraction grating material the intensity of incident light was approximately 15mw and the output intensity is approximately 8.5mw. The output intensity was stable with respect to time.
3. For the master radial grating the incident light was approximately 15mw and the output intensity was approx 7.5mw. The output is very stable with respect to time.

4.2 FOR THE FIRST ORDERED DIFFRACTED BEAM:

1. For PTP type of diffraction grating material. Average intensity of the first ordered diffracted beam is 3.053mw.
2. For CSG type of diffraction grating material. Average intensity of the first ordered diffracted beam is 3.08mw
3. For the master radial grating the average intensity of first order diffracted beam approximately 7mw.

5. DISCUSSIONS AND CONCLUSION

We reviewed physical basis of the particle and optical channeling phenomena in crystals and artificial periodic structures. Theoretical modeling of the optical channeling in periodic two-dimensional structures is briefly described. Feasibility of the optical channeling for recording of the radial grating in the chalcogenide glassy semiconductor films was demonstrated. Optical channeling explains recreation of the

periodic phase structure for the volume grating. For thin phase grating, recreation of the periodic structure in the near field is described by the Talbot effect. These two effects, channeling and Talbot, may be both used for description of intermediate case between volume and thin gratings (that is the case for some of our gratings).

ACKNOWLEDGEMENTS

This work has been done with the support of the Title 111 program, CRDF grant (award number ME2-2317-CH-02), and DOE/HU Sub #633254-HC1C060

References

1. J.B.Bond and J.S Williams, Eds, Ion beams for Material Analysis (Academic Press, 1989).
2. J.F.Ziegler, J.P.Biersack and U. Littmark, The Stopping and Range of Ions in Solids (Pergamon, N.Y. 1985)
3. O.Konstantinov, I.Shmulevich, Channeling of light in a medium with a periodically varying refractive index, Sov. Phys.Solid State, **24**, 1817, (1983)
4. R.Rupp, Investigation of the Dynamic recording Process of Thick Refractive Index Gratings in Photorefractive Crystals by the Microphotometric Method, Appl.Phys. **B42**, 21 (1987)
5. S.Solimeno, B.Crosignani, P.Di Porto, Guiding, Diffraction and Confinement of Optical Radiation, Academic Press, Inc. New York, pp104-106, (1986)
6. N.Kukhtarev, T.Kukhtareva, D.Ila, E.Williams, R.Zimmerman, J.Caulfield, Channeling in LiNbO₃:Fe Modulated by Holographic Stress Field Superlattice, Mat. Res. Symp. Proc., Vol. 316, (1994)
7. V.I.Vysotskii and R.N.Kuzmin, Channeling of neutral particles and photons in crystals, Sov.Phys, Usp, 25(9), 725 (1992)
8. V.D.D.Jabon, G.V.Fedorovich and N.V.Samsonenko, Catalytically Induced D-D Fusion in Ferroelectrics, Braz.J.Phys, vol.27, n.4, p.1, (1997)
9. N.Kukhtarev, T.Kukhtareva, H.J.Caulfield, A. Knyazkov, Two dimensional optical channeling, Optik, 97, No.1, 7-8, (1994)
10. N.Kukhtarev, T.Kukhtareva, H.J.Caulfield, and A.Knyazkov, "Channeling of Photons on Holographic Gratings" Optik, **8**, 1154, (1994)
11. R.M. Shaffert, *Electrophotography*, Wiley, New York, 1975.
12. L.M. Panasyuk, "Formation of the charge image on electrophotographic layers of vitreous chalcogenide semiconductors in different recording regimes," *Sov. J. Opt. Technol.* **58**, 725-729 (1991).
13. L.M. Panasyuk, S.I. Kovtunencko, "Photographic systems based on the semiconductors with charged free-surface," *Sov. J. Sci. Appl. Photogr.* **33**, 307-317 (1988).
14. V.L. Averyanov, B.T. Kolomiets, V.M. Lyubin, G.A. Fedorova, "Localized states in chalcogenide vitreous semiconductors," *Phys. Stat. Sol. A* **22**, K105-K107 (1974).
15. E. Spear, "Electronic transport and localization in low mobility solids and liquids," *Adv. Phys.* **23**, 523-546 (1974).
16. D.L. Wood, J. Tauc, "Weak optical absorption tails in amorphous semiconductors," *Phys. Rev. B* **5**, 3144-3151 (1972)
17. Davis, N.F. Mott, "Conduction in non-crystalline systems: 5. Conductivity, optical absorption and photoconductivity in amorphous semiconductors," *Philos. Mag.* **22**, 903-922 (1970).

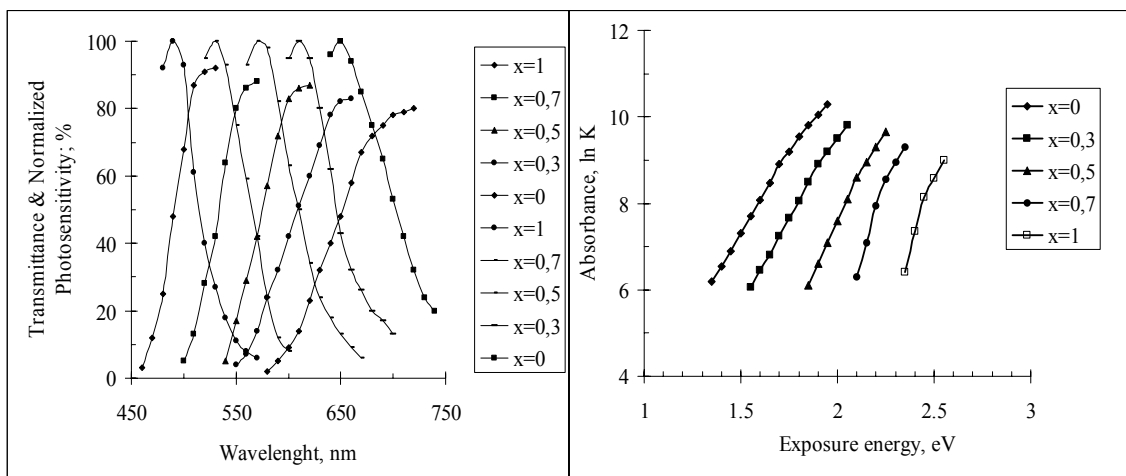


Fig.1. Interrelations between transmittance and normalized photosensitivity for $(As_2S_3)_x(As_2Se_3)_{1-x}$ layers.

Fig.2. Dependence of the $(As_2S_3)_x(As_2Se_3)_{1-x}$ system absorption on photon energy of incident irradiation.

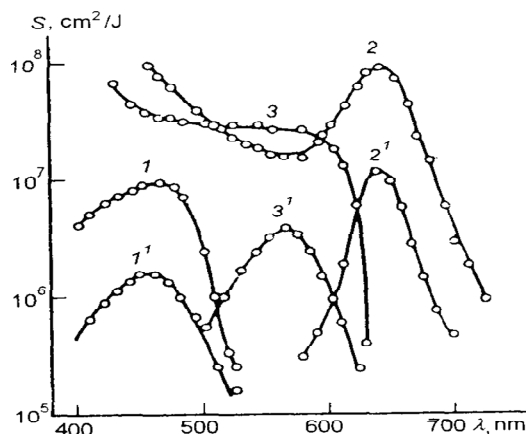


Fig.3. Spectral sensitivity of PTPF based on: As_2S_3 (1, 1'); As_2Se_3 (2, 2'); $(As_2S_3)_{0.3}(As_2Se_3)_{0.7}$ (3, 3').

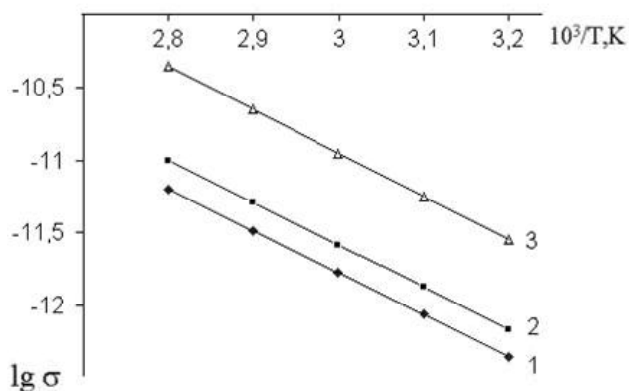


Fig.4. Thermal dependence of the conductivity of As-S-Se-Sn thin layers: 1- 10^4 ; 2- $4 \cdot 10^4$; 3- $8 \cdot 10^4$ V/cm.

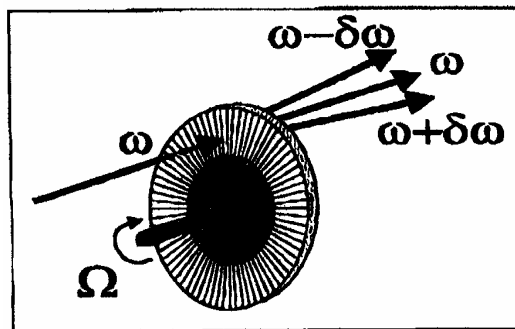
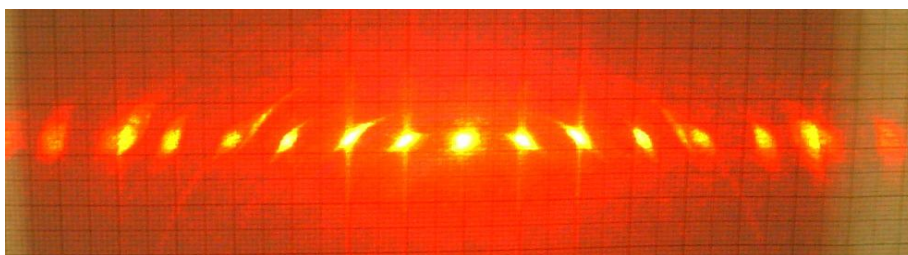
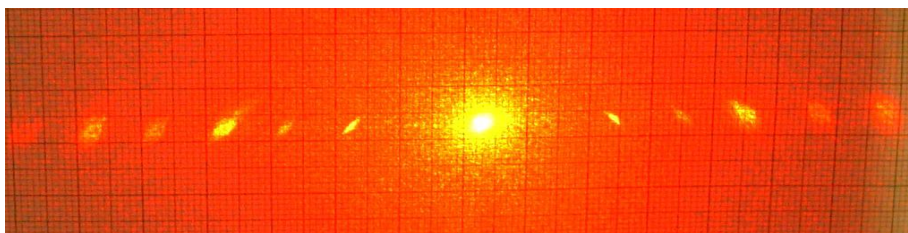


Fig.5. Photo of the radial grating. Rotation of this grating allows to introduce angular shift in the diffracted beams.



(a)



(b)

Fig. 6. Diffraction orders in (a) master grating, and (b) grating recorded in CGS.

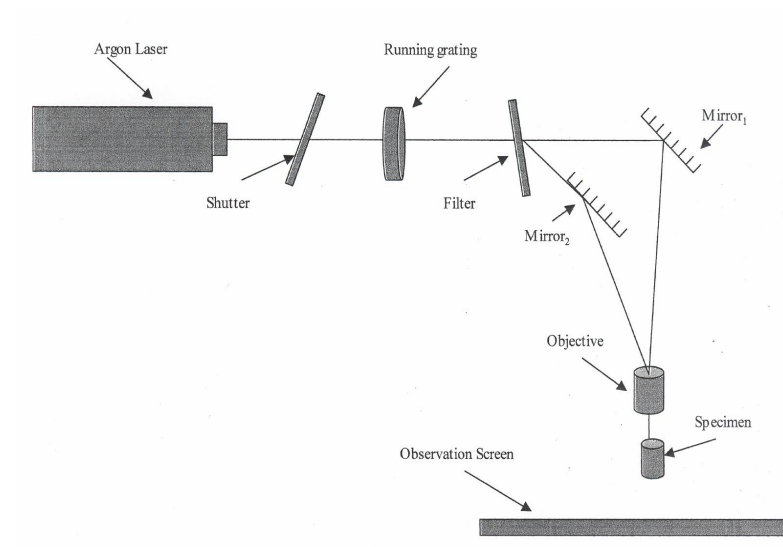


Fig.7. Experimental setup for creation of moving interference pattern with rotating radial grating